13th World Conference on Earthquake Engineering
Vancouver, B.C., Canada
August 1-6, 2004
Paper No. 3139

FULL SCALE PSEUDODYNAMIC EARTHQUAKE TESTS ON A THREE-STORY URM BUILDING USING SUB-STRUCTURE-TECHNIQUE

Konrad ZILCH[1], Detleff SCHERMER[2]

SUMMARY

To investigate the behavior of unreinforced masonry (URM) constructions under seismic loading full-scale pseudo-dynamic tests have been carried out. The tested structure has been reduced to a symmetric and plane 3-DOF system. The tests were carried out just on the relevant shear wall in the first story under combined vertical and horizontal loadings. The upper two stories of the structure with the shear-walls and their restraint in the concrete slabs considered numerically modeled as a sub-structure. Its stiffness characteristics in the shape of nonlinear bending- and shear-springs were determined within preceding static-cyclic tests. The evaluation of the results focused on the stiffness and load reduction. It can be concluded that unreinforced masonry structures show a significantly better behavior under seismic loadings than determined by current codes.

INTRODUCTION

According to the new European Earthquake Standard Eurocode 8 seismic loads increase significantly in regions of low seismicity, e.g. Central Europe. Combined with the proposed behavior factor q=1.5 the earthquake resistance of several common types of unreinforced masonry buildings can't be proven numerically.

To investigate the seismic behavior of unreinforced masonry constructions under realistic conditions, tests on full scale masonry walls were necessary. Within these experiments the load bearing capacity under combined shear / normal stress and also the load-deformation behavior were tested.

The chosen pseudo-dynamic test method allowed considering the characteristics of regions of low seismicity, e.g. the earthquake duration and the frequency range of the seismic input resp. the response spectra.

[1] Professor, Head of the Institute of Concrete and Masonry Structures, Technical University Munich, Germany. Email: k.zilch@mb.bv.tum.de

[2] Dipl.-Ing., Head of the Masonry Research Group at the Institute of Concrete and Masonry Structures, Technical University Munich, Germany. Email: schermer@mb.bv.tum.de

INVESTIGATE STRUCTURE

The investigations of Zilch / Schermer [1], [2], [3] focused on commonly used masonry constructions with few bracing shear walls. These types of buildings are composed of concrete slabs – distributing the horizontal loads – and vertical unreinforced masonry (URM) walls, carrying the vertical and also the horizontal loads. For the tested masonry walls the given materials in table 1 were used.

Table 1 Materials of the walls

Wall [1)]	Description	Unit dimensions	Used mortar type
A, B, C, D	vertically perforated lightweight bricks type a) – f_b = 12N/mm² 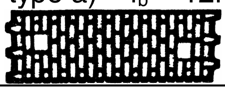	495 mm * 175 mm * 238 mm	cement-lime mortar
E, F	vertically perforated lightweight bricks type b) – f_b = 12N/mm² 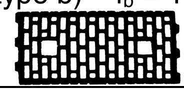	378 mm * 175 mm * 247 mm	thin-layer mortar (wall E) cement-lime mortar (wall F)
KS1, KS2	sandlime blocks – f_b=20 N/mm² 	998 mm * 175 mm * 498 mm	thin-layer mortar
KS3, KS4	sandlime bricks – f_b=20 N/mm² 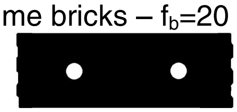	499 mm * 175 mm * 248 mm	thin-layer mortar with varying adhesion between mortar and units (KS3, KS4)
[1)] Walls A, B and C tested in the first series; [2)] Secant stiffness			

Table 2 Survey of the tested walls

Wall	Execution	Wall dimensions	Perpend joints
A, B, C, D	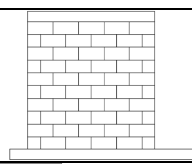	250 cm * 250 cm * 17,5 cm	unfilled
E, F[1)]	E: 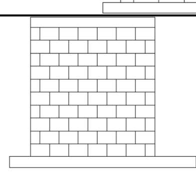 F: 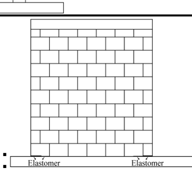	243 cm * 250 cm * 17,5 cm	unfilled
KS1, KS2	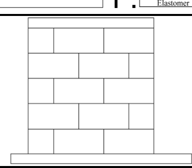	250 cm * 250 cm * 17,5 cm	unfilled (wall KS1) resp. filled (wall KS2)
KS3, KS4	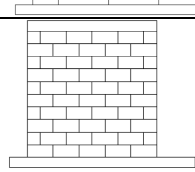,	250 cm * 250 cm * 17,5 cm	unfilled
[1)] Wall F with elastomer plates 200 mm * 175 mm * 8 mm & 200 mm * 175 mm * 5 mm in the bottom corners			

Reduction and Sub-Structure

In the described 2nd test series a unit of a 3-storey terraced house was investigated (figure 1). For simplification the structure was reduced to a plane multi-degree-of-freedom system with elastic restraint in the concrete slabs.

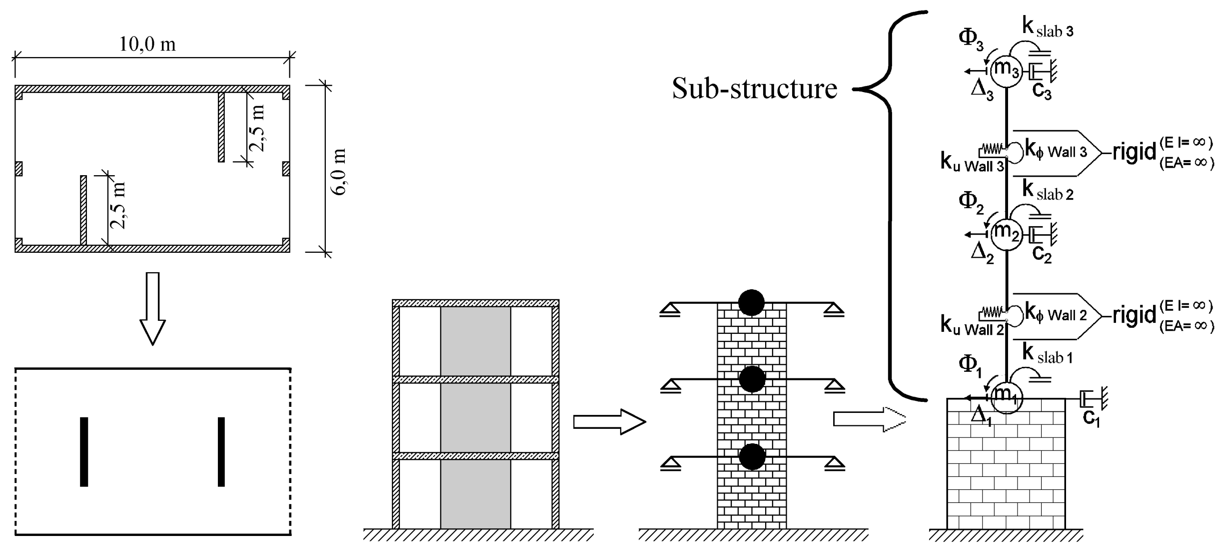

Figure 1 Structure with reduction to a plane multi-degree-of-freedom system and substitution of the upper two stories by a sub-structure – 2nd series

The total deformation $\underline{\Delta}$ (figure 1 / 2) vector is condensed to

$$\underline{\Delta} = \begin{Bmatrix} \Delta_1 - \Delta_0 \\ \Delta_2 - \Delta_0 \\ \Delta_3 - \Delta_0 \end{Bmatrix} = \begin{bmatrix} 1 & \frac{h_1}{2} & 0 & 0 & 0 & 0 \\ 1 & \frac{h_1}{2} + h_2 & 1 & \frac{h_2}{2} & 0 & 0 \\ 1 & \frac{h_1}{2} + h_2 + h_3 & 1 & \frac{h_2}{2} + h_3 & 1 & \frac{h_3}{2} \end{bmatrix} \cdot \underline{d} \qquad (1)$$

with $\underline{d} = \{u_1 \quad \varphi_{1rel} \quad u_2 \quad \varphi_{1rel} \quad u_3 \quad \varphi_{3rel}\}^T$

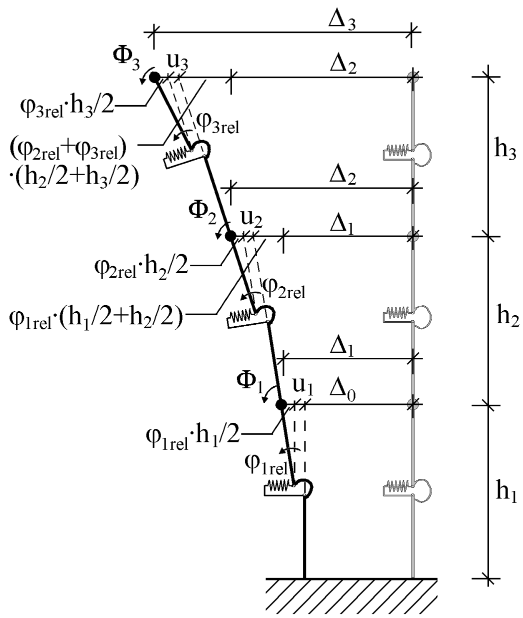

Figure 2 Kinematics

The tests were carried out just on the relevant shear wall in the first story. The structure of the upper two stories with the shear-walls and their restraint in the concrete slabs were modeled as a sub-structure. Its stiffness characteristics in the shape of nonlinear bending- and shear-springs were determined within preceding static-cyclic tests.

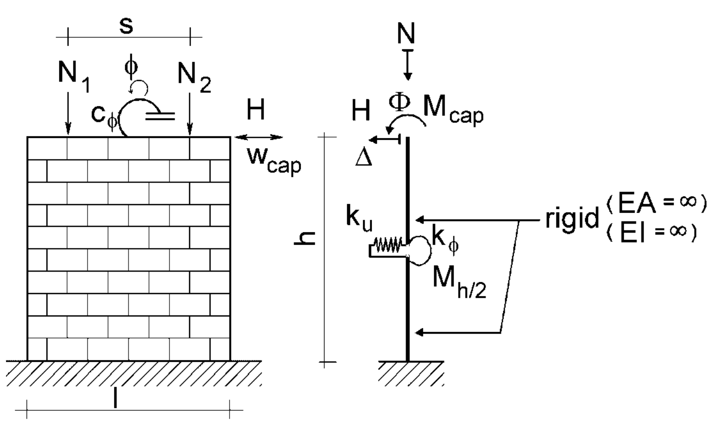

Figure 3 System of the preceding tests and substitution by non-linear shear- and bending-springs

In the preceding tests (see figure 3) the normal force $N = N_1 + N_2$ was varied in the range of the normal forces in the 3 stories, i.e. in levels of 90, 180 and 270kN. The tests were carried out under static-cyclic horizontal loads. Adapting boundary conditions as found in real structures, the appearing cap rotation (ϕ resp. Φ) was restricted by the application of a bending spring $c_\phi = M_{cap} / \phi$ at the cap of the wall. Its stiffness within these preceding tests was also varied in a range of 0 (M_{cap} =0) ÷ ∞(c_ϕ=0) to cover the possible stress-states in the sub-structure. The bending moment at the cap of the wall $M_{cap} = (N_1 - N_2)*s/2$ was applied by two computer-controlled hydraulic actuators through different normal forces N_1 and N_2.
For the description of the stiffnesses k_ϕ and k_u the command variable was taken to be the associated relative rotation Φ and the relative displacements Δ resp. moment loading in the middle of the wall $M_{h/2}$ (wall D).

Table 3 Stiffness characteristics of the sub-structure

Wall [1]	**k_{u2}** [2] **[kN/mm]**	**k_{u3}** [2] **[kN/mm]**	**$k_{\phi 2}$** [2] **[kNm/mrad]**	**$k_{\phi 3}$** [2] **[kNm/mrad]**
D	70:$\|M_{h/2}\|$=0kNm 35:$|M_{h/2}||\geq$45kNm (type 1) [3]	47:$\|M_{h/2}\|$=0kNm 23:$|M_{h/2}|\geq$80kNm (type 1) [3]	≡ 200	≡ 125
E	≡ 60	≡ 45	≡ 200	130:$\|\Phi\|$=0mrad 60:$|\Phi| \geq$0,8mrad (type 2) [3]
F	≡ 42	35:$\|\Delta\|$=0mm 25:$|\Delta| \geq$2mm (type 2) [3]	≡ 80	55:$\|\Phi\|$=0mrad 28:$|\Phi| \geq$1,5mrad (type 2) [3]
KS1	≡ 220	≡120	≡ 320	220:$\|\Phi\|$=0mrad 120:$|\Phi| \geq$0,4mrad (type 2) [3]
KS2	330:$|\Delta| \leq$0,1mm 200:$|\Delta| \geq$0,4mm (type 3) [3]	170:$\|\Delta\|$=0mm 100:$|\Delta| \geq$0,5mm (type 2) [3]	400:$|\Phi| \leq$0,1mrad 310:$|\Phi| \geq$0,2mrad (type 3) [3]	250:$\|\Phi\|$=0mrad 120:$|\Phi| \geq$0,25mrad (type 2) [3]
KS3; KS4	≡ 260	180:$\|\Delta\|$=0mm 135:$|\Delta| \geq$0,4mm (type 2) [3]	400:$\|\Phi\|$=0mrad 300:$|\Phi| \geq$0,23mrad (type 2) [3]	230:$\|\Phi\|$=0mrad 140:$|\Phi| \geq$0,35mrad (type 2) [3]

[1] walls A, B and C tested in the first series; [2] secant stiffness
[3]

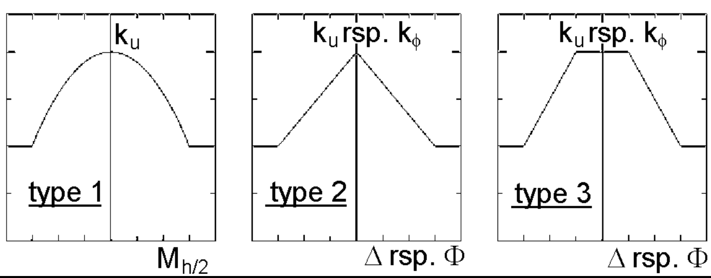

For restraint in the concrete slabs the constant spring stiffness k_{slab} was determined considering stiffness reduction by cracks.

Damping

To cover additional damping effects due to several material and structural effects in the structure three single viscous dampers in the levels of the storey masses were arranged. The values $c_{1,2,3}$ were determined according to the target damping rate of 5% of the whole structure

MAIN TESTS

All tests were carried out at the laboratories of the Institute of Concrete and Masonry Structures at the Technical University Munich (www.mb.bv.tum.de). The normal force and the cap moment were applied by two independent computer-controlled hydraulic actuators, arranged between the roller bearing on top of the concrete cap beam and the horizontal girder of the test frame. The horizontal cap-displacements were applied also by a computer-controlled hydraulic actuator with a high accuracy of 4/100 mm. To avoid any restraint effects at horizontal load application, in the middle of the cap beam a moment hinge in the shape of a steel bolt was arranged.

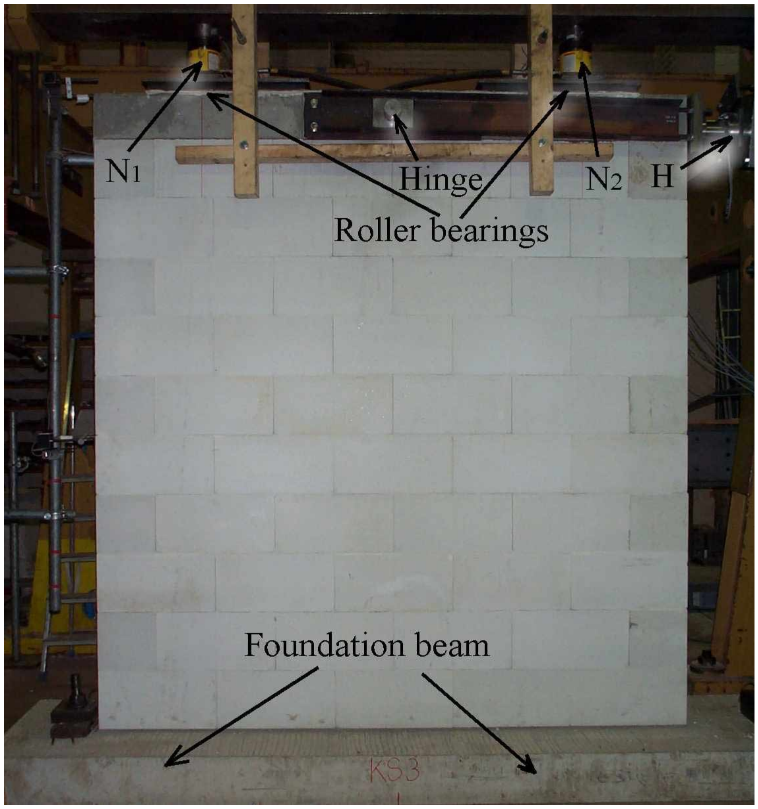

Figure 4 Test arrangement

Measurements

Displacements in all relevant points and also the horizontal restoring force H and the vertical forces N_1 and N_2 were measured during the tests continuously with a frequency of 50 Hz. The data were displayed during the test real-time on a screen.

Time histories

The time histories used were generated artificially adjusted to the response spectra of the new German Earthquake Code DIN 4149 (2002-10) resp. Eurocode 8. The intensity function and the total earthquake duration were adapted to the conditions in regions of low seismicity in Central Europe. During the tests of each wall the seismic load level was increased stepwise in each test with a load-level factor f.

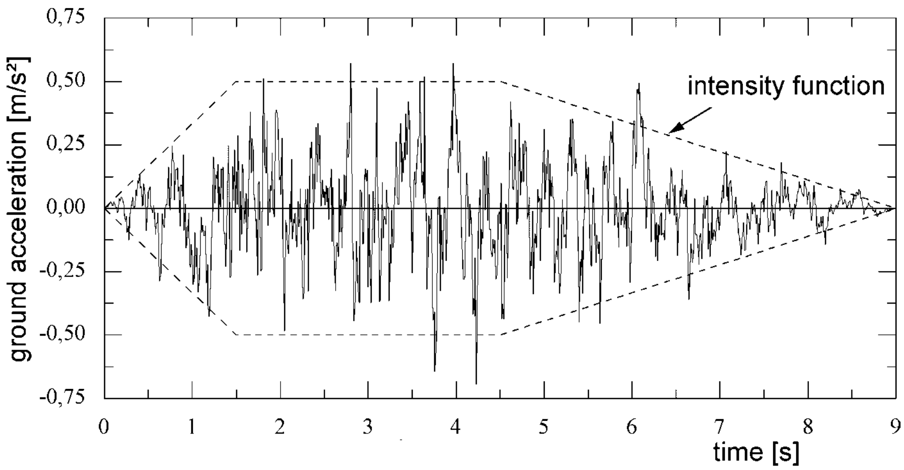

Figure 5 Time history ZV1 with intensity function (load-level factor f=1)

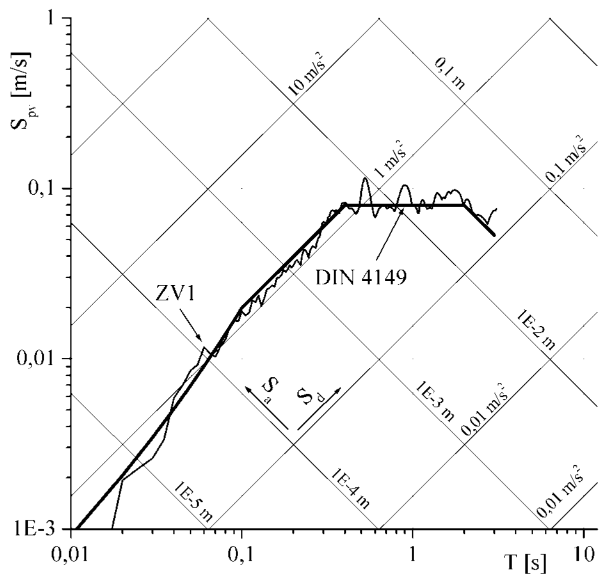

Figure 6 Response spectra of time history ZV1 with corresponding target spectrum of DIN 4149

Time integration method

In the pseudo-dynamic test-method the equation of motion (2) has to be solved in each time step. For the numerical integration the implicit α-method (4), described by Hilber / Hughes / Taylor [4] based on the Newmark (3) method, was used.

$$\underline{m} \cdot \underline{a} + \underline{c} \cdot \underline{v} + \underline{r}(\underline{d}) = -\underline{m} \cdot \underline{a}^g \tag{2}$$

$$\underline{d}_{n+1} = \underline{d}_n + \underline{v}_n \cdot \Delta t + \left[\left(\frac{1}{2} - \beta\right) \cdot \underline{a}_n + \beta \cdot \underline{a}_{n+1}\right] \cdot \Delta t^2 \tag{3a}$$

$$\underline{v}_{n+1} = \frac{\gamma}{\beta \cdot \Delta t} \cdot \left(\underline{d}_{n+1} - \underline{d}_n\right) - \left(\frac{\gamma}{\beta} - 1\right) \cdot \underline{v}_n - \Delta t \cdot \left(\frac{\gamma}{2 \cdot \beta} - 1\right) \cdot \underline{a}_n \tag{3b}$$

$$\underline{a}_{n+1} = \frac{1}{\beta \cdot \Delta t^2} \cdot (\underline{d}_{n+1} - \underline{d}_n) - \frac{1}{\beta \cdot \Delta t} \cdot \underline{v}_n - \left(\frac{1}{2 \cdot \beta} - 1\right) \cdot \underline{a}_n \tag{3c}$$

$$\begin{aligned} &\underline{m}_{ges} \cdot \underline{a}_{n+1} + (1+\alpha) \cdot \underline{c}_{ges} \cdot \underline{v}_{n+1} - \alpha \cdot \underline{c}_{ges} \cdot \underline{v}_n - \alpha \cdot \underline{k}_{ges} \cdot \underline{d}_n \\ &+ (1+\alpha) \cdot \underline{k}_{ges} \cdot \underline{d}_{n+1} = -(1+\alpha) \cdot \underline{m}_{ges} \cdot \underline{a}^g_{n+1} + \alpha \cdot \underline{m}_{ges} \cdot \underline{a}^g_n \end{aligned} \tag{4}$$

The parameter α, β and γ were determined to:

$$\alpha = -\frac{1}{3} \qquad \beta = \frac{(1-\alpha)^2}{4} = \frac{4}{9} \qquad \gamma = \frac{1}{2} - \alpha = \frac{5}{6}$$

Due to the high numerical effort for measurements and controlling, two standard personal computers had to be used. The first computer had to measure, control the actuators and also to display the results real-time on the screen. The second computer carried out the implicit time integration. For a fast data exchange a serial connection-cable was used. The total duration of the test was about 70 minutes.

RESULTS

Stiffness degradation

Carrying out a linear-elastic calculation of the horizontal wall-stiffness taking E-modulus from literature resp. design codes leads to significantly higher values than appeared in the tests. The relation is between 1.5 and 3.3 (in the 1st story with N = 270kN) and between 3.0 and 5.9 (in the 3rd story with N = 90kN). Generally a high dependency on the normal force and the effect of opening bed-joints was found.

To describe the wall-stiffness focusing only on the load-displacement-relation (H-w_{cap}-hystersis) leads to improper results. In addition, the bending stiffness and the co-action with the horizontal displacements have to be considered. As a consequence, for further investigations the stiffness of the whole structure was calculated from the time-displacement-history. The 1st eigenperiod $T_{1,FFT}$ was calculated by applying the fast-fourier-analysis to the displacement-history in the first storey Δ_1.

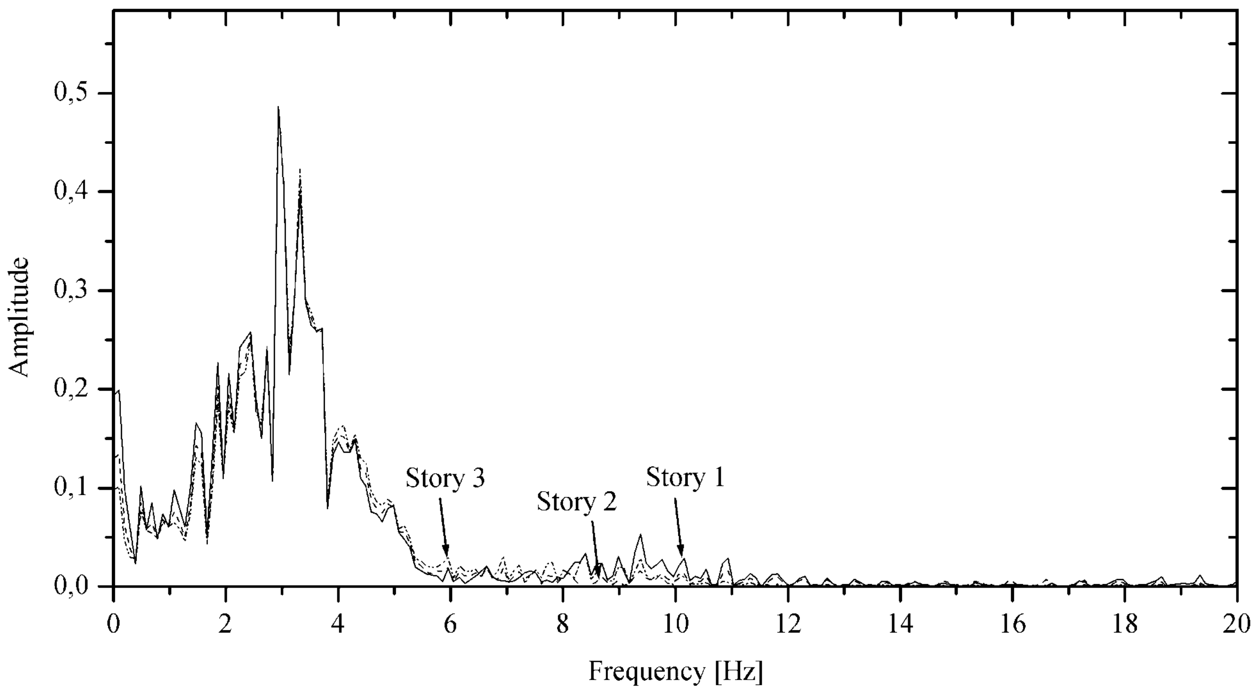

Figure 7 Determination of the eigenperiods in the test KS1-7 using the fast-fourier-analysis – 2nd series

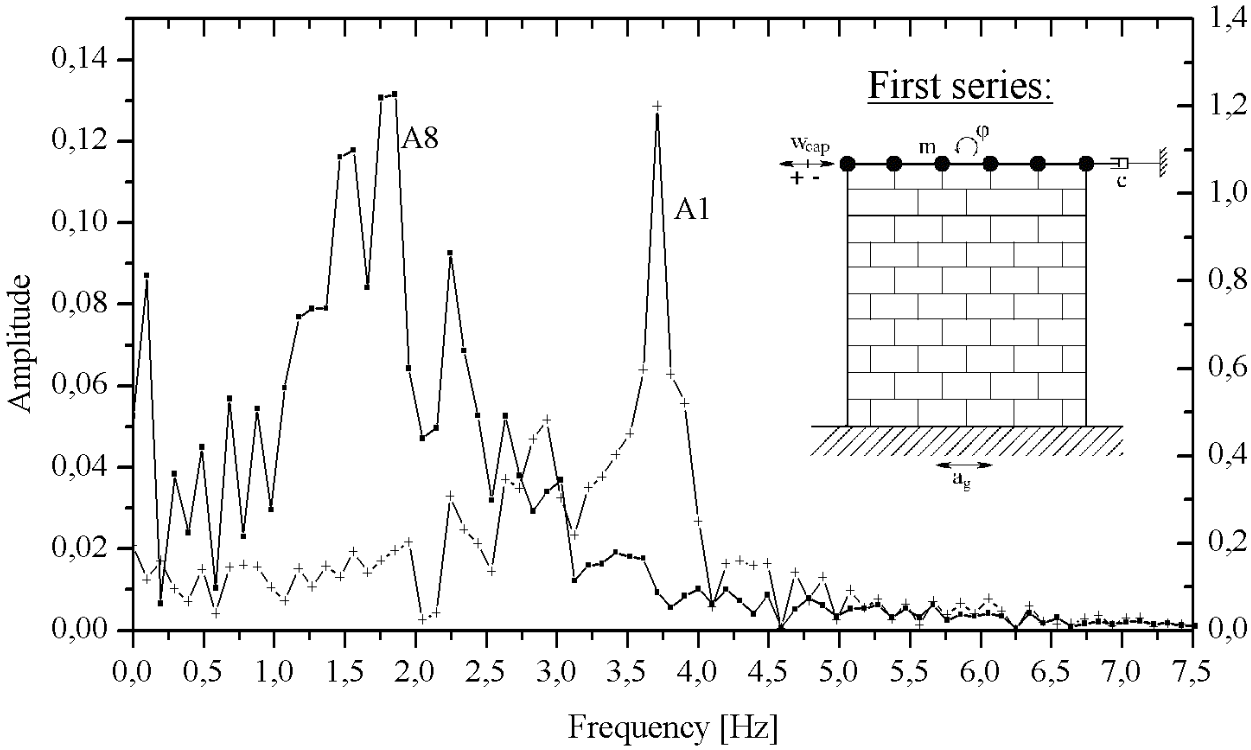

Figure 8 Change of the eigenperiods in the test A1 (f=0.25) and A8 (f=2.16) – 1st series

For comparison as reference value the first eigenperiod $T_{1,elastic}$ calculated on an linear elastic system using the maximum stiffness values under minimal stress (initial stiffness, table 3) has

been taken. A meaningful example is the relation between the tests A1 and A8 in the first series (SDOF-system), shown in figure 8.
The illustration in figure 9 shows the dependence on the load level, calculated from the relation of maximum measured horizontal force in the mentioned test and the maximum horizontal force of all test of the investigated wall.

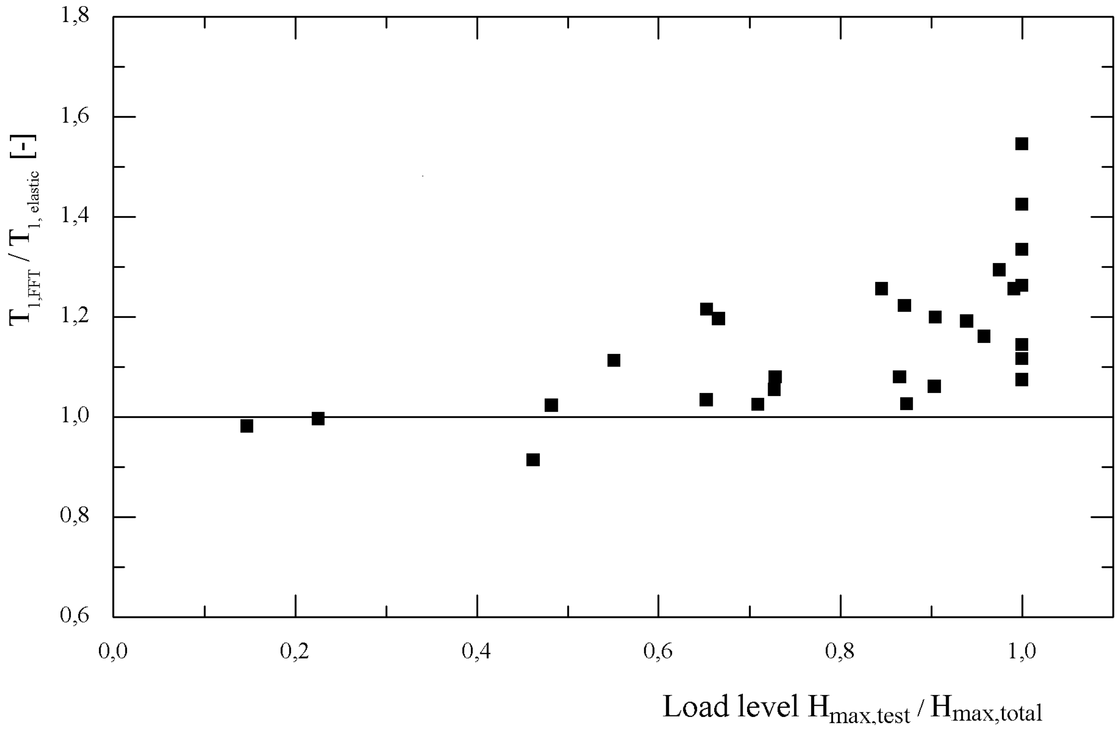

Figure 9 Stiffness reduction in the tests versus load level – 2nd series

The stiffness degradation at the maximum load level were between 1.07 and 1.55 (mean value 1.27).

Load reduction

In current seismic codes, the linear-elastically calculated horizontal loads are usually reduced for design with the behavior-factor q. Generally for unreinforced masonry q = 1.5 is given, e.g. in Eurocode 8.
In the presented tests, with the initial system-stiffness in a first step a linear calculation of the whole system has been carried out. The resulting theoretical maximum horizontal forces H_{calc} were then compared to the maximum forces appeared in the tests H_{test}. The illustration of this ratio takes place against the load level, calculated from the ratio of maximum appeared horizontal force in the mentioned test $H_{max,test}$ and the maximum horizontal force of all test of the investigated wall $H_{max,wall}$. Additional in figure 10 the ratio of maximum cap displacement observed in the tests $w_{cap,test}$ and the result of a linear-elastic calculation with initial stiffness $w_{cap,calc.}$ is shown.

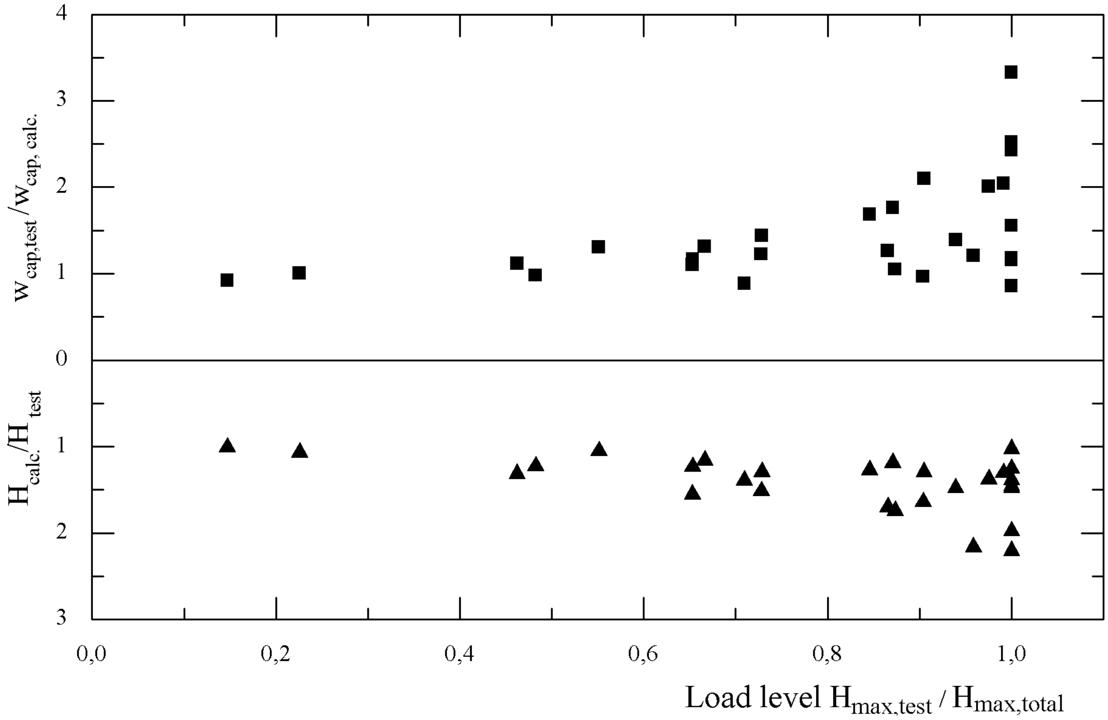

Figure 10 Load reduction and displacement enhancement in the tests versus load level – 2nd series

In conjunction with the rising load level, the reduction of the calculational horizontal load and the increasing calculational cap displacement grow. The ratio of H_{calc}/H_{test} averages 1.42 (range 1.0 ÷ 2.21) - slightly less than $w_{cap,test}/w_{cap,calc.}$ found to 1.46 (range 0.86 ÷ 3.33). At the maximum load level the ratio of $H_{calc.}/H_{test}$ ranges from 1.03 (KS2-2) to 2.21 (KS1-7) (mean value 1,54) and the ratio of $w_{cap,test}/w_{cap,calc.}$ ranges from 0.86 (D-4) to 3.3 (KS4-4) (mean value 1.86).

Load-bearing capacity

The comparison of observed maximum horizontal loads and maximum loads according to the design code DIN 1053-1 showed significant load-bearing reserves. In table 4 the summary of the results of the 2nd series is shown.

Table 4 Maximum horizontal loads and cap displacements in the tests – 2nd series

Wall / Test	Initial stiffness [1), 2)] $k_{\phi,i}$ [kNm/mrad] $k_{u,i}$ [kN/mm]	Damper [1)] $c_{,,i}$ [kNs/m]	Time history [3)]; Load factor f [-]	Maximum cap displacement w_{cap} [mm]	Maximum horizontal load H [kN]]
D-1	275; 200; 125 100; 70; 47	172,5; 2,8; 13,1	ZV1-B3 (a_g=0,4m/s²) f=0,15	0,33	22,8
D-2			f=1	2,11	109,9
D-3			f=1,5	3,46	140,0
D-4			f=2	4,11	154,9
D-5			f=2,67	4,52 [4)]	145,5 [4)]
E-1	270; 200; 130 80; 60; 45	35; 1; 4,3	ZV4-C3 (a_g=0,4m/s²) f=1	1,5	61,8
E-2			f=2,67	4,27 [4)]	112,1 [4)]
F-1	120; 80; 55 50; 42; 35	240; 70; 6	ZV3-A1 (a_g=0,4m/s²) f=2	1,85	55,7
F-2			ZV4-C3 (a_g=0,4m/s²) f=3	5,37	115,4
F-3			ZV3-A1 (a_g=0,4m/s²) f=7	8,0 [4)]	110,6 [4)]
KS1-1	470; 320; 220 300; 220; 120	700; 60; 40	ZV3-A1 (a_g=0,4m/s²) f=2	0,87 [4)]	76,6 [4)]
KS1-2		525; 200; 0	f=2	1,18	108,2
KS1-3			f=3	1,68	144,7
KS1-4		570; 85; 30	f=3	1,76 [4)]	120,7 [4)]
KS1-5			f=3	1,74	120,6
KS1-6			f=4	2,40	143,4
KS1-7			f=6	3,36	165,7
KS1-8			f=8	3,21 [4)]	149,9 [4)]
KS2-1	470; 400; 250 400; 330; 170	700; 60; 40	ZV3-A1 (a_g=0,4m/s²) f=1	0,37	47,3
KS2-2			f=8	3,62 [4)]	209,4 [4)]
KS3-1	500; 400; 230 350; 260; 180	675; 45; 50	ZV1-B3 (a_g=0,4m/s²) f=1,5	1,26	117,3
KS3-2			f=2	2,24	153,3
KS3-3			f=2,5	3,25	174,5
KS3-4			f=3,5	3,88 [4)]	176,0 [4)]
KS4-1	500; 400; 230 350; 260; 180	675; 45; 50	ZV1-B3 (a_g=0,4m/s²) f=1,5	1,12	110,6
KS4-2			f=2	2,14	143,2
KS4-3			f=2,5	3,19	165,1
KS4-4			f=3,5	5,42 [4)]	169,3 [4)]

1) Restraint in bending springs $k_{slab,i}$ =300 kNm/mrad (except: KS1-2 & 1-3: 600);
h = 2,60 m; 3 single story masses: $m_{1,2,3}$ = 29 t

2) Non-linear stiffness characteristics $k_{\phi,i}$ and $k_{u,i}$: s. table 3

3) Time history, Soil-subsoil-conditions; ground acceleration

4) Test stopped premature

LOAD-DISPLACEMENT-CURVES

In the following figure 11 the hysteresis of the tests under maximal loads are displayed.

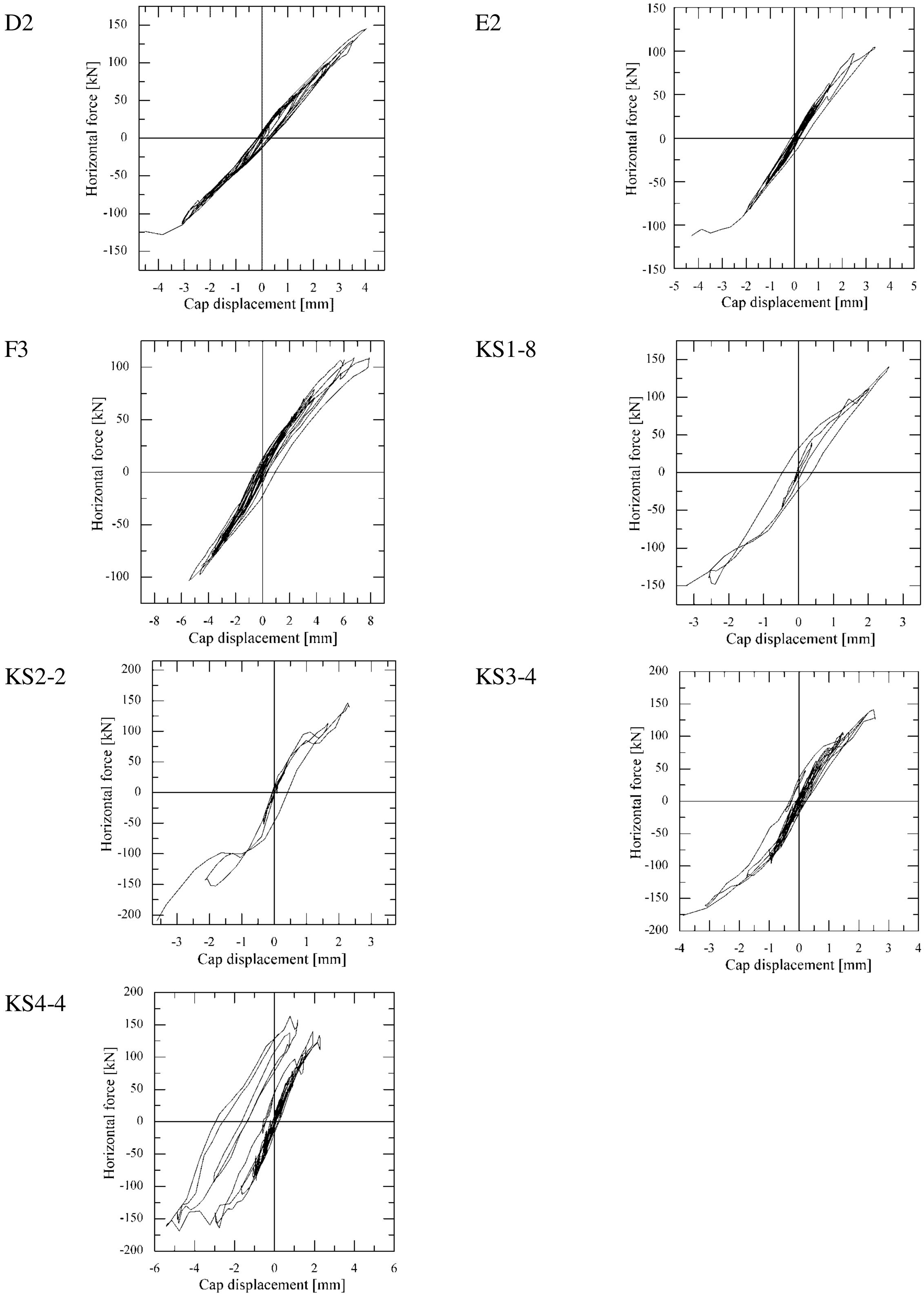

Figure 11 Hysteresis of the tested walls D – F and KS1 – KS4 at maximum load level

CRACK PATTERN

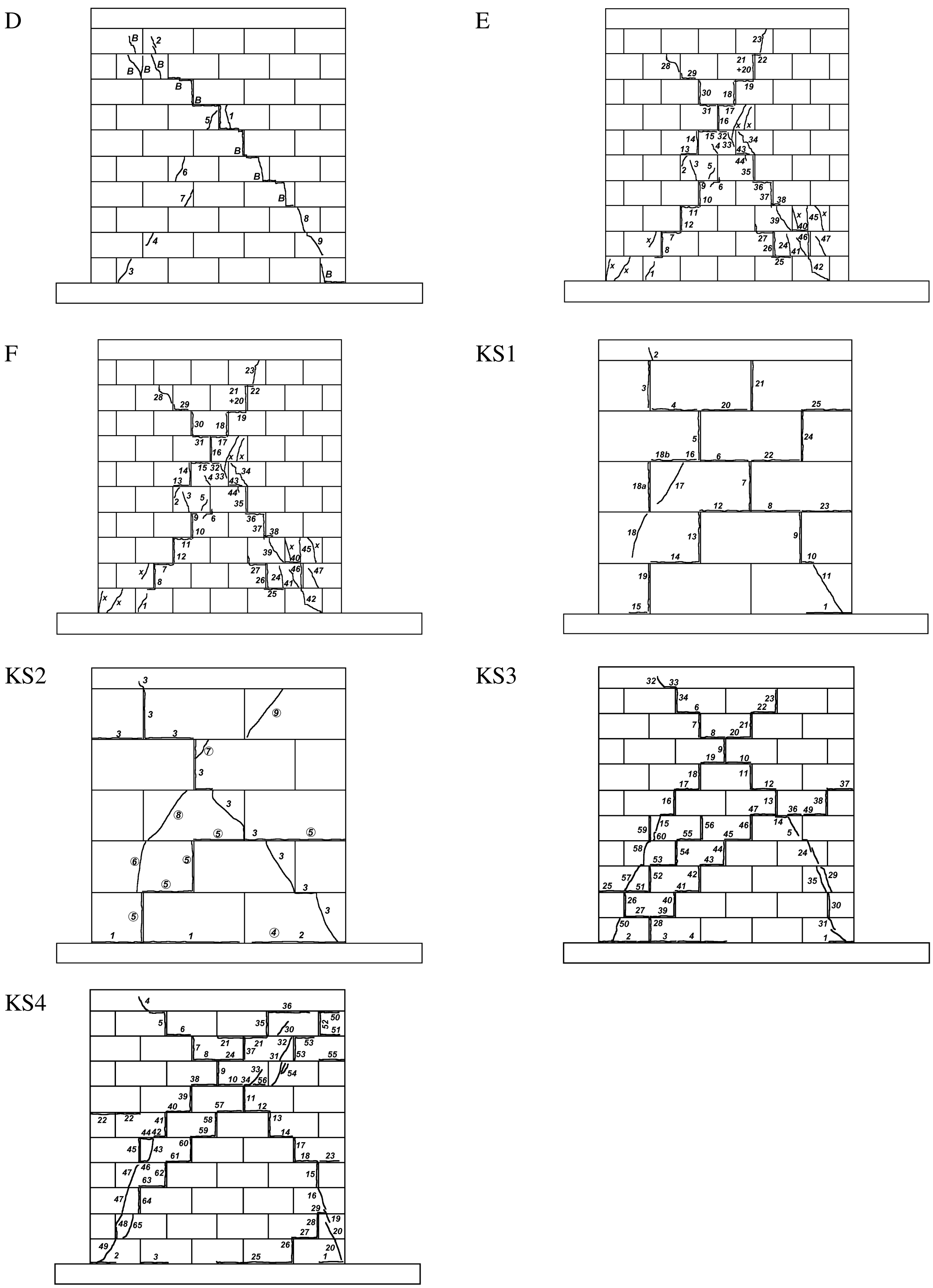

Figure 12 Crack pattern of the tested walls D – F and KS1 – KS4

CONCLUSIONS

For the investigation of MDOF-system under dynamic loadings the pseudo-dynamic test method with sub-structure technique may be recommended. The chosen implicit time integration method led to fast and stable results. Totally in the 2nd series (3-DOF-system) 28 and in the 1st series (SDOF-system) 12 main tests and numerous preceding tests have been performed. As a result of the experimental investigations it can be concluded, that partially a higher behavior factor than given in current codes as q = 1.5 is justifiable for URM. Under the mentioned conditions, i.e. investigated seismic load level, normal stress level, brick-mortar-combination and mechanical boundary conditions, behavior factor up to 2.0 can be postulated.

Also the load bearing capacity under lateral loadings was significantly higher than expected according to the design codes. Further research will focus on the dynamic behavior of wall systems with t-shaped cross section and the material optimization.

REFERENCES

[1] Zilch, K.; Schermer, D.; Scheulfer, W.: Simulated Earthquake Behavior of Unreinforced Masonry Walls, In: Grundmann (Ed.): EUORDYN 2002, Munich 2002.

[2] Schermer, D.: Verhalten von unbewehrtem Mauerwerk unter Erdbebenbeanspruchung. Dissertation TU Munich (in German language / to be published / www.mb.bv.tum.de), 2003.

[3] Zilch, K.; Schermer, D., 2004: Experimentelle und numerische Untersuchungen zum Erdbebentragverhalten unbewehrter Mauerwerksbauten, In: Schubert (Ed.): Mauerwerk-Kalender 2004, pp. 649-664 (in German language). Ernst & Sohn, Berlin.

[4] Hilber, H. M.; Hughes, T. J. R.; Taylor, R. L.: Improved numerical dissipation for time integration algorithms in structural dynamics, In: Earthquake engineering and structural dynamics, 1977.